

Crystalline Polyphenylene Covalent Organic Frameworks

Xing Han, Zihui Zhou, Kaiyu Wang, Zhiling Zheng, S. Ephraim Neumann, Heyang Zhang, Tianqiong Ma, and Omar M. Yaghi*



Cite This: <https://doi.org/10.1021/jacs.3c11688>



Read Online

ACCESS |



Metrics & More



Article Recommendations



Supporting Information

ABSTRACT: The synthesis of crystalline polyphenylene covalent organic frameworks (COFs) was accomplished by linking fluorinated tris(4-acetylphenyl)benzene building units using aldol cyclotrimerization. The structures of the two COFs, reported here, were confirmed by powder X-ray diffraction techniques, Fourier transform infrared, and solid-state ^{13}C CP/MAS NMR spectroscopy. The results showed that the COFs were porous and chemically stable in corrosive, harsh environments for at least 1 week. Accordingly, postsynthetically modified derivatives of these COFs using primary amines showed CO_2 uptake from air and flue gas.

The chemistry of covalent organic frameworks (COFs) has been largely dominated by structures made from highly reversible linkages such as imines,^{1–4} boroxines,^{5,6} and hydrazones.^{7,8} Recently, COFs containing linkages considered irreversible have also been successfully crystallized, most notably, olefins,^{9–11} sp^2 -carbon,^{12–15} truxenes,¹⁶ triazines,^{17–19} phenazines,^{20,21} oxazoles,^{22,23} and dioxins.^{24–26} An important objective is to crystallize COFs based on C–C linkages so that such structures could be deployed for many years in capturing carbon dioxide from air and flue gas, among many applications. We report the use of aldol cyclotrimerization (Figure 1) to form polyphenylene COFs.

Specifically, the cyclotrimerization of 1,3,5-trifluoro-2,4,6-tris(4-acetylphenyl)benzene (TAB) or 1,3,5-trifluoro-2,4,6-tris(4-acetylphenylethynyl)benzene (TAEB) yields crystalline 2D frameworks with hcb topology, termed COF-284 and COF-285 (Figures 1b and 1c). The phenyl linkages of these COFs were unambiguously confirmed by Fourier transform infrared (FTIR) spectroscopy and solid state ^{13}C cross-polarization magic angle spinning (CP-MAS) NMR spectroscopy. The irreversible phenyl linkage endows the COFs with exceptionally high stability under extreme chemical conditions. Following postsynthetic modification, alkyl amines can be anchored onto the backbone of the COFs, resulting in a CO_2 uptake capacity at low pressure (0.4 mbar).

The molecular reaction of aldol cyclotrimerization of the acetophenone has been used to synthesize a variety of molecules and polymers (e.g., 1,3,5-triphenylbenzene, TPB, Figures 1a and S1). The reaction is typically performed in the presence of a strong Brønsted acid.^{27,28} However, applying these reaction conditions directly to the synthesis of COFs leads to the expected formation of amorphous materials, indicating insufficient reversibility for defect correction.^{29,30} Extensive efforts were applied to screen various synthetic conditions, including linkers, solvent mixtures, temperature, and reaction time. For reactions that exhibit irreversible characteristics and therefore lack the ability to self-correct defects, careful modulation of the reaction conditions is crucial

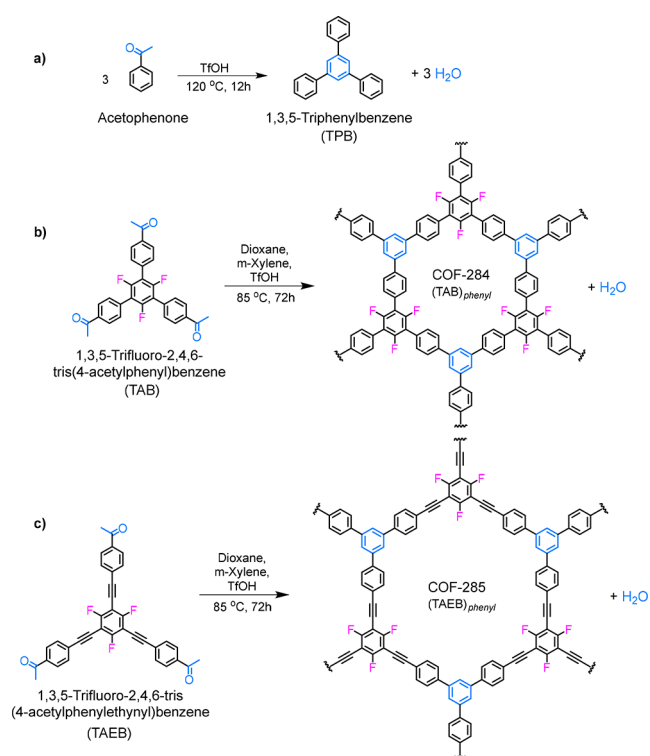


Figure 1. (a) Aldol cyclotrimerization by acetophenone yielded the model compound TPB. (b, c) Synthesis of COF-284 and COF-285 by aldol cyclotrimerization with the fluorinated linkers TAB and TAEB.

Received: October 19, 2023

Revised: December 11, 2023

Accepted: December 13, 2023

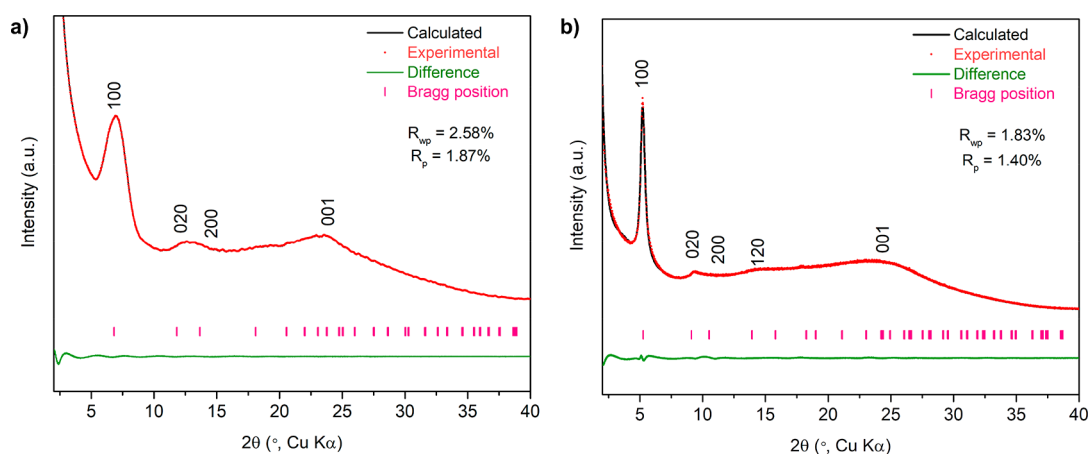


Figure 2. PXRD patterns and Pawley refinement of COF-284 (a) and COF-285 (b), respectively. The experimental pattern (red) is in good agreement with that of the eclipsed stacking model (black).

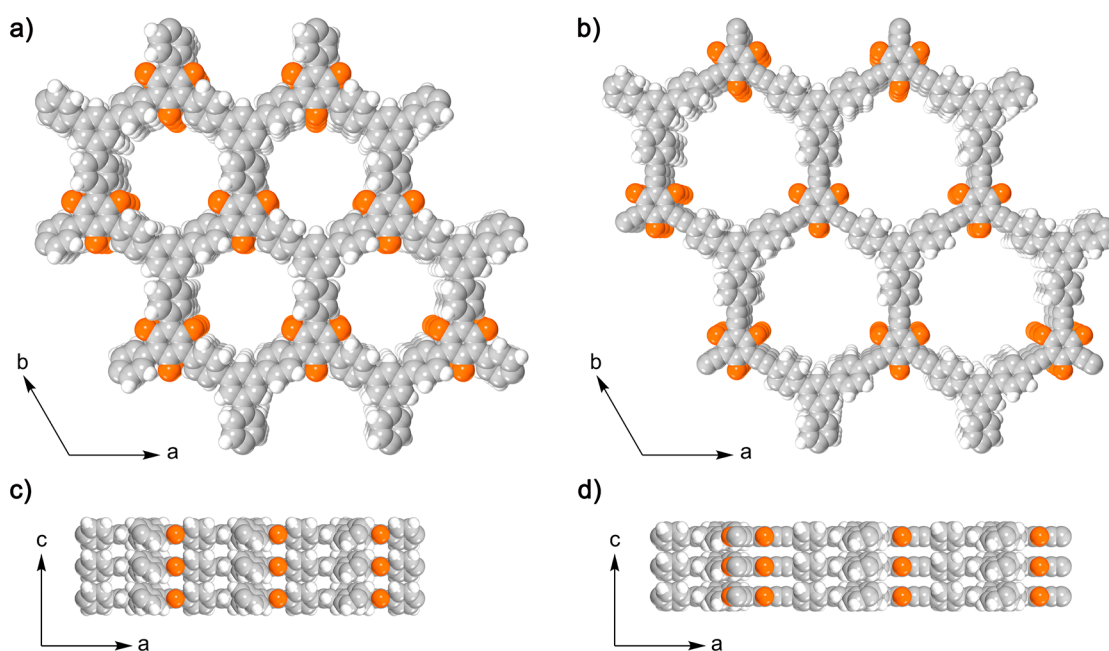


Figure 3. (a, b) Top views and (c, d) side views of the space-filling models of COF-284 and -285 in eclipsed stacking mode. Color code: H, white; C, gray; and F, orange.

to reduce the reaction rate. This ensures that linkers connect slowly enough to assemble and stack in an orderly fashion, thus yielding a crystalline structure. However, a common trade-off with this approach is a potential reduction in the reaction yield. A crystalline framework, termed COF-284, was successfully synthesized under solvothermal conditions in a mixture of 1,4-dioxane, and *m*-xylene, with aqueous trifluoromethanesulfonic acid (TfOH) as a catalyst at 85 $^\circ\text{C}$ for 72 h in moderate yield (32%) (Section S2.6).

In this process, we employed a two-pronged strategy for synthesizing COF-284. Initially, we conducted a human-centric screening, which was later augmented with a machine learning (ML) guided approach for optimizing the synthesis conditions. This methodology efficiently identifies optimal conditions from a potentially vast space of combinations derived from seven key synthesis parameters (Section S2.10). The ML component involved the Bayesian Optimization (BO) algorithm,^{31–36} known for efficiently sampling parameters to find a global optimum in minimal steps.³⁷ The implementation

of the BO process begins by defining an objective function, in our case, the crystallinity of the studied COF, and builds a surrogate model over the vast experimental space defined by synthesis parameters. These include a myriad of combinations involving choices of solvents and modulators, their respective volumes, linker amounts, reaction times, and temperature. The combinations stemmed from seven key synthesis parameters hypothesized to influence the crystallinity of the resulting COF-284 (Tables S1 and S2).³⁸ In particular, a random forest (RF) model was used as the surrogate model due to its capacity to handle both the continuous synthesis parameters and the categorical parameters, such as the choice of solvent and modulator. Utilizing an acquisition function, Expected Improvement (EI), the algorithm strikes a balance between exploiting areas of a high predicted objective and exploring areas of high uncertainty. The iterative process within the Bayesian Optimization framework, which involves updating the model with each batch of experiments, enhances its efficiency in suggesting synthesis conditions that yield optimal

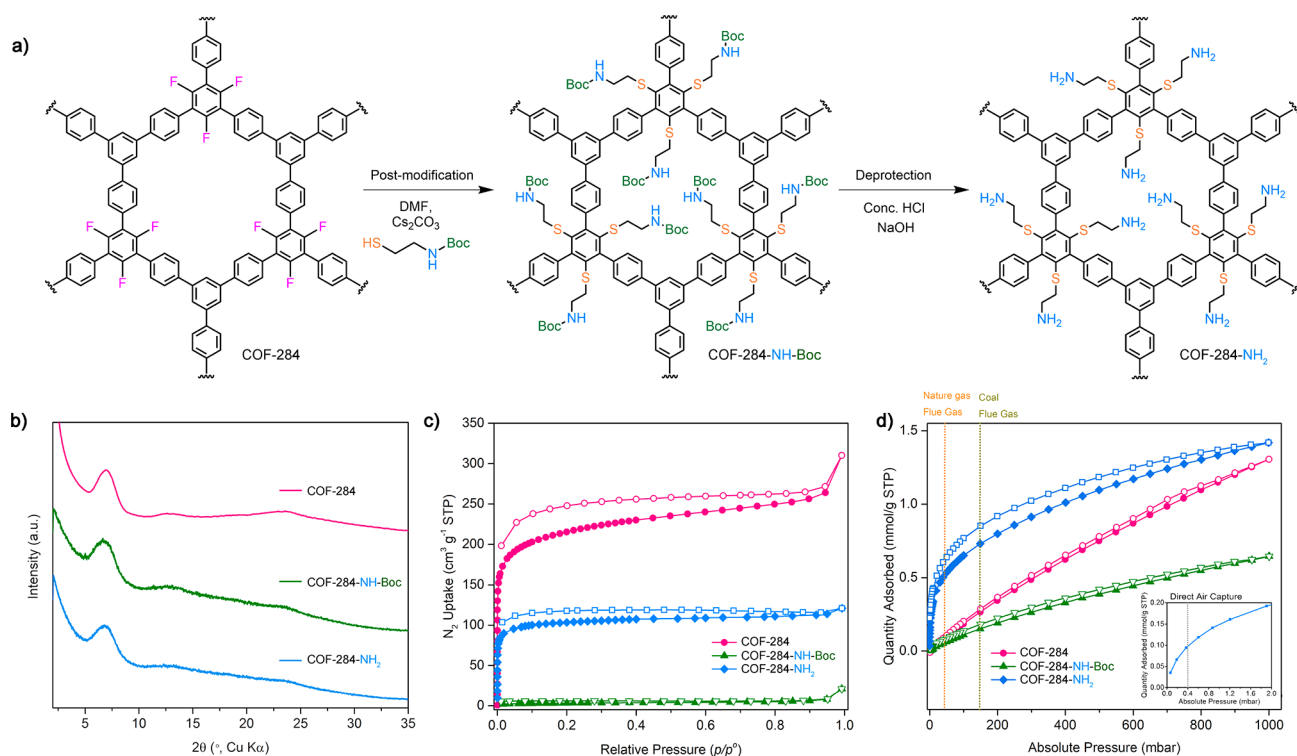


Figure 4. (a) Schematics of the synthesis of COF-284-NH₂, (b) PXRD patterns, (c) N₂ sorption isotherms (77 K), and (d) single component CO₂ isotherms (25 °C) of COFs. The inset of panel (d) shows a zoomed-in view of the adsorption branch for COF-284-NH₂ between 0 and 2 mbar, highlighting the uptake at the pressure range relevant for DAC (Direct Air Capture).

crystallinity parameters (Section S2.10). This method simultaneously reduces human bias and adeptly balances the dual needs of exploration and exploitation in the search for optimal conditions (Figure S2).

We further extended the reaction scope by crystallizing COF-285 through the cyclotrimerization of TAEB using similar conditions. COF-285 demonstrates improved crystallinity compared to COF-284. This enhancement is attributed to the acetylene groups present in COF-285, which reduce steric repulsion and consequently facilitate the crystallization process. COF-284 and -285 were obtained as pale-yellow microcrystalline powders, insoluble in common organic solvents such as dichloromethane, acetone, *N,N*-dimethylformamide, alcohols, and tetrahydrofuran. It should be noted that incorporating fluorine substituents onto the periphery of the building units of the COFs plays an important role in the ability to crystallize these structures. We hypothesized that fluorine being an electron-withdrawing group enhances aromatic stacking interactions without introducing significant steric effects.³⁹ The nonfluorinated analogous building blocks only form amorphous solids under similar synthetic conditions (Figure S19).

In the FTIR spectra of COF-284 and COF-285, the peaks attributed to the C=O and C–H stretching of the acetyl linkers, found at approximately 1680 and 3040 cm⁻¹, respectively, are markedly reduced compared to the spectra of TAB and TAEB (Figures S3 and S4). Concurrently, there is an increased intensity at approximately 1600 to 1605 cm⁻¹, corresponding to the aromatic C=C stretch in the phenyl ring formed during the COF synthesis. The residual C=O stretch at 1686 to 1688 cm⁻¹ can be assigned to the defects and intermediates formed during the COF's synthesis. Further support for the presence of the phenyl linkages was obtained

by solid-state ¹³C cross-polarization magic angle spinning (CP-MAS) NMR analysis. The ¹³C CP-MAS NMR spectra of COF-284 and COF-285 revealed the almost complete disappearance of signals at chemical shifts of 195 and 25 ppm, which correspond to the carbonyl and alkyl carbons of the acetyl group, respectively (Figures S7 and S8). Although there is an overlap of aromatic carbon signals between the linkage and the backbone, an increased peak intensity at 126 ppm was observed, which is attributed to the newly formed phenyl rings.

The crystallinity of COF-284 and COF-285 was confirmed by Powder X-ray diffraction (PXRD) (Figure 2). Structural models of COF-284 and COF-285 were constructed using an *hcb* topology, guided by the planar geometry observed in the model compound TPB and its analogs within single-crystal structures (Figure 3). A variety of interlayer stacking modes were simulated and then compared to the experimental PXRD pattern. Among these, the model featuring an eclipsed (AA) stacking mode in the *P3* space group showed the best fit (Figures S17 and S18). Full profile Pawley refinement of the model against the experimental pattern yielded a unit cell parameters of $a = b = 14.98 \text{ \AA}$ and $c = 4.01 \text{ \AA}$, $\alpha = \beta = 90^\circ$, $\gamma = 120^\circ$ with good agreement factors ($R_{wp} = 2.58\%$, $R_p = 1.87\%$) for COF-284 and $a = b = 19.44 \text{ \AA}$ and $c = 3.65 \text{ \AA}$, $\alpha = \beta = 90^\circ$, $\gamma = 120^\circ$ with agreement factors ($R_{wp} = 1.83\%$, $R_p = 1.40\%$) for COF-285, respectively.

The porosity and surface areas of COF-284 and COF-285 were evaluated following the removal of solvent molecules from the pores by activation *in vacuo*. The N₂ sorption isotherm measurements performed on COF-284 and COF-285 at 77 K revealed that the pores of the two COFs were accessible to N₂, with a Brunauer–Emmett–Teller (BET) surface area of 812 m² g⁻¹ and 395 m² g⁻¹, respectively (Figures 4c, S21 and S22). The analysis of the isotherm using

nonlocal density functional theory revealed a uniform pore size distribution in COF-284 and COF-285, characterized by narrow peaks at diameters of 9.2 and 12.6 Å, respectively, which closely align with the expected diameters of 9.3 and 13.0 Å, as predicted from the calculated van der Waals surface of the structural model (Figure S23).

The thermal stability of COF-284 and COF-285 was evaluated using thermogravimetric analysis. Both COFs exhibited high thermal stability, showing no significant weight loss up to 400 °C under a N₂ atmosphere (Figures S13 and S14). The chemical stability of the polyphenylene COFs was tested by exposing the materials to various organic and inorganic Brønsted acids and bases. Specifically, the activated COFs were immersed in solutions of 12.1 mol L⁻¹ aqueous HCl (35 wt %), trifluoromethanesulfonic acid (≥99%), H₂SO₄ (98 wt %), saturated aqueous KOH (55 wt %), and saturated methanolic KOH (35 wt %), and maintained at room temperature for a duration of 1 week. The structural integrity of the treated COF powders was examined by PXRD (Figure 5). The framework structures were found to maintain their

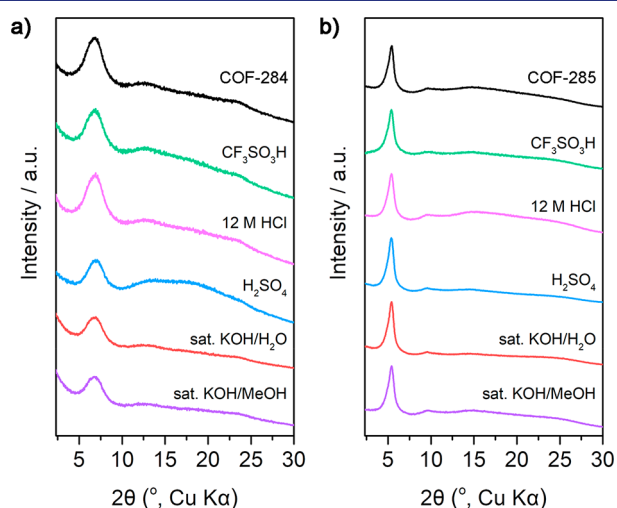


Figure 5. Chemical stability test of (a) COF-284 and (b) COF-285 with Brønsted acid and base. PXRD patterns of treated materials illustrate the retention of the crystallinity of COFs under these very harsh conditions.

crystallinity under all conditions. This is demonstrated by the observation that the PXRD patterns of all of the treated samples largely retained their shape and intensity. Notably, the stability of the COFs in aqueous acid or base solutions can also be attributed to the hydrophobic nature of the materials. As such, COF-284 and COF-285 were suspended in pure TfOH, H₂SO₄, and saturated solutions of KOH in methanol, in which the materials still retained their crystallinity. The fact that the two COFs remain intact even under such harsh conditions for this length of time suggests significant chemical stability.

To utilize the exceptional stability and accessible fluorine functionalities, we developed a postsynthetic modification process to generate open amine groups within the pores of COF-284 and COF-285 (Figure 4a). The fluoride groups undergo a substitution reaction with 2-(Boc-amino) ethanethiol that decorates the channel walls with Boc-protected alkyl amines (Figures S5, S6, S9, and S10). The COFs-NH-Boc can be readily deprotected using HCl, which results in the exposure of the corresponding amines, producing COFs-

NH₂. The PXRD patterns of the postmodified COF-284 exhibited a minor reduction in crystallinity, as shown in Figure 4b, whereas the postmodified COF-285 completely lost its crystallinity (Figure S20). The apparent decrease in the N₂ isotherm of COFs-NH-Boc can be attributed to the introduced functional groups that block the pores of the framework (Figures 4c and S21). After the Boc group was deprotected during the amination step, the porosity of material was partially restored, resulting in a BET surface area of 401 m² g⁻¹ and 272 m² g⁻¹ for COF-284-NH₂ and COF-285-NH₂, respectively.

Single-component CO₂ sorption isotherms of COFs before and after postmodification were measured at 25 °C and compared as shown in Figures 4d and S25. In the case of COF-284, the absence of a sharp increase in uptake at low pressures and minimal hysteresis suggested that the framework exhibits physisorption-dominant characteristics. COF-284-NH-Boc exhibited lower CO₂ uptake in the entire range of experiment (0–1000 mbar), which was attributed to the blocked pores after postmodification. In contrast, the CO₂ sorption isotherm for COF-284-NH₂ showed a sharp increase in the adsorption branch at very low CO₂ pressures. This was followed by a more moderate slope between 50 and 1000 mbar along with a noticeable hysteresis between the adsorption and desorption branches. Specifically, COF-284-NH₂ and COF-285-NH₂ adsorb 2.2 cm³ g⁻¹ STP (0.10 mmol g⁻¹) and 1.5 cm³ g⁻¹ STP (0.07 mmol g⁻¹) at 0.4 mbar CO₂ (conditions relevant to DAC), respectively (Figures 4d, the inset and S25), whereas COF-284, COF-285, and COF-284-NH-Boc, COF-285-NH-Boc isotherms, as expected, did not take up any CO₂ at such a low concentration. It should be noted that, at a pressure of 40 mbar, which is relevant for postcombustion capture from natural gas flue gas, COF-284-NH₂ adsorbs 11.2 cm³ g⁻¹ at standard temperature and pressure (STP), equivalent to 0.5 mmol g⁻¹ of CO₂. This represents a 6-fold increase compared to COF-284, which adsorbs 1.79 cm³ g⁻¹ STP or 0.08 mmol g⁻¹ of CO₂ under the same conditions. Additionally, at 150 mbar, relevant to postcombustion capture from coal flue gas, the CO₂ uptake of COF-284-NH₂ is 16.6 cm³ g⁻¹ STP (0.74 mmol g⁻¹), which is three times higher than that of COF-284, with an uptake of 5.6 cm³ g⁻¹ STP (0.25 mmol g⁻¹). The substantial enhancement in CO₂ uptake strongly suggests that introducing chemisorption by incorporating aliphatic amines into COFs indicates their promising potential as efficient sorbents for DAC and postcombustion CO₂ capture (Figures S11 and S12).

■ ASSOCIATED CONTENT

SI Supporting Information

The Supporting Information is available free of charge at <https://pubs.acs.org/doi/10.1021/jacs.3c11688>.

Detailed experimental section, Characterization including XRD, FTIR, solid-state NMR, and TGA (PDF)

Accession Codes

CCDC 2301434–2301435 contain the supplementary crystallographic data for this paper. These data can be obtained free of charge via www.ccdc.cam.ac.uk/data_request/cif, or by emailing data_request@ccdc.cam.ac.uk, or by contacting The Cambridge Crystallographic Data Centre, 12 Union Road, Cambridge CB2 1EZ, UK; fax: +44 1223 336033.

■ AUTHOR INFORMATION

Corresponding Author

Omar M. Yaghi – Department of Chemistry and Kavli Energy Nanoscience Institute, University of California, Berkeley, California 94720, United States; Bakar Institute of Digital Materials for the Planet, College of Computing, Data Science, and Society, University of California, Berkeley, California 94720, United States; KACST–UC Berkeley Center of Excellence for Nanomaterials for Clean Energy Applications, King Abdulaziz City for Science and Technology, Riyadh 11442, Saudi Arabia; orcid.org/0000-0002-5611-3325; Email: yaghi@berkeley.edu

Authors

King Han – Department of Chemistry and Kavli Energy Nanoscience Institute, University of California, Berkeley, California 94720, United States; Bakar Institute of Digital Materials for the Planet, College of Computing, Data Science, and Society, University of California, Berkeley, California 94720, United States; orcid.org/0000-0002-7921-8197

Zihui Zhou – Department of Chemistry and Kavli Energy Nanoscience Institute, University of California, Berkeley, California 94720, United States; Bakar Institute of Digital Materials for the Planet, College of Computing, Data Science, and Society, University of California, Berkeley, California 94720, United States

Kaiyu Wang – Department of Chemistry and Kavli Energy Nanoscience Institute, University of California, Berkeley, California 94720, United States; Bakar Institute of Digital Materials for the Planet, College of Computing, Data Science, and Society, University of California, Berkeley, California 94720, United States

Zhilong Zheng – Department of Chemistry and Kavli Energy Nanoscience Institute, University of California, Berkeley, California 94720, United States; Bakar Institute of Digital Materials for the Planet, College of Computing, Data Science, and Society, University of California, Berkeley, California 94720, United States; orcid.org/0000-0001-6090-2258

S. Ephraim Neumann – Department of Chemistry and Kavli Energy Nanoscience Institute, University of California, Berkeley, California 94720, United States; Bakar Institute of Digital Materials for the Planet, College of Computing, Data Science, and Society, University of California, Berkeley, California 94720, United States; orcid.org/0000-0002-8515-9621

Heyang Zhang – Department of Chemistry and Kavli Energy Nanoscience Institute, University of California, Berkeley, California 94720, United States; Bakar Institute of Digital Materials for the Planet, College of Computing, Data Science, and Society, University of California, Berkeley, California 94720, United States

Tianqiong Ma – Department of Chemistry and Kavli Energy Nanoscience Institute, University of California, Berkeley, California 94720, United States; Bakar Institute of Digital Materials for the Planet, College of Computing, Data Science, and Society, University of California, Berkeley, California 94720, United States

Complete contact information is available at:
<https://pubs.acs.org/10.1021/jacs.3c11688>

Notes

The authors declare no competing financial interest.

■ ACKNOWLEDGMENTS

This research was supported by King Abdulaziz City for Science and Technology (KACST) as part of a joint KACST–UC Berkeley Center of Excellence for Nanomaterials for Clean Energy Applications. The authors thank Drs. Hasan Celik, Raynald Giovine, and UC Berkeley's NMR facility in the College of Chemistry (CoC-NMR) for spectroscopic assistance. The instrument used in this work is supported by the National Science Foundation under Grant No. 2018784 and NIH S10OD024998. The authors thank the University of California Berkeley Electron Microscope Laboratory for access and assistance in electron microscopy data collection.

■ REFERENCES

- (1) Ding, S.-Y.; Gao, J.; Wang, Q.; Zhang, Y.; Song, W.-G.; Su, C.-Y.; Wang, W. Construction of Covalent Organic Framework for Catalysis: Pd/COF-LZU1 in Suzuki–Miyaura Coupling Reaction. *J. Am. Chem. Soc.* **2011**, *133* (49), 19816–19822.
- (2) Natraj, A.; Ji, W.; Xin, J.; Castano, I.; Burke, D. W.; Evans, A. M.; Strauss, M. J.; Ateia, M.; Hamachi, L. S.; Gianneschi, N. C.; Althman, Z. A.; Sun, J.; Yusuf, K.; Dichtel, W. R. Single-Crystalline Imine-Linked Two-Dimensional Covalent Organic Frameworks Separate Benzene and Cyclohexane Efficiently. *J. Am. Chem. Soc.* **2022**, *144* (43), 19813–19824.
- (3) Ma, T.; Kapustin, E. A.; Yin, S. X.; Liang, L.; Zhou, Z.; Niu, J.; Li, L.-H.; Wang, Y.; Su, J.; Li, J.; Wang, X.; Wang, W. D.; Wang, W.; Sun, J.; Yaghi, O. M. Single-crystal x-ray diffraction structures of covalent organic frameworks. *Science* **2018**, *361* (6397), 48–52.
- (4) Sun, T.; Wei, L.; Chen, Y.; Ma, Y.; Zhang, Y.-B. Atomic-Level Characterization of Dynamics of a 3D Covalent Organic Framework by Cryo-Electron Diffraction Tomography. *J. Am. Chem. Soc.* **2019**, *141* (28), 10962–10966.
- (5) Côté, A. P.; Benin, A. I.; Ockwig, N. W.; O'Keeffe, M.; Matzger, A. J.; Yaghi, O. M. Porous, Crystalline, Covalent Organic Frameworks. *Science* **2005**, *310* (5751), 1166–1170.
- (6) El-Kaderi, H. M.; Hunt, J. R.; Mendoza-Cortés, J. L.; Côté, A. P.; Taylor, R. E.; O'Keeffe, M.; Yaghi, O. M. Designed Synthesis of 3D Covalent Organic Frameworks. *Science* **2007**, *316* (5822), 268–272.
- (7) Uribe-Romo, F. J.; Doonan, C. J.; Furukawa, H.; Oisaki, K.; Yaghi, O. M. Crystalline Covalent Organic Frameworks with Hydrazone Linkages. *J. Am. Chem. Soc.* **2011**, *133* (30), 11478–11481.
- (8) Stegbauer, L.; Schwinghammer, K.; Lotsch, B. V. A hydrazone-based covalent organic framework for photocatalytic hydrogen production. *Chem. Sci.* **2014**, *5* (7), 2789–2793.
- (9) Xu, J.; He, Y.; Bi, S.; Wang, M.; Yang, P.; Wu, D.; Wang, J.; Zhang, F. An Olefin-Linked Covalent Organic Framework as a Flexible Thin-Film Electrode for a High-Performance Micro-Supercapacitor. *Angew. Chem., Int. Ed.* **2019**, *58* (35), 12065–12069.
- (10) Lyu, H.; Diercks, C. S.; Zhu, C.; Yaghi, O. M. Porous Crystalline Olefin-Linked Covalent Organic Frameworks. *J. Am. Chem. Soc.* **2019**, *141* (17), 6848–6852.
- (11) Wei, S.; Zhang, F.; Zhang, W.; Qiang, P.; Yu, K.; Fu, X.; Wu, D.; Bi, S.; Zhang, F. Semiconducting 2D Triazine-Cored Covalent Organic Frameworks with Unsubstituted Olefin Linkages. *J. Am. Chem. Soc.* **2019**, *141* (36), 14272–14279.
- (12) Chen, R.; Shi, J.-L.; Ma, Y.; Lin, G.; Lang, X.; Wang, C. Designed Synthesis of a 2D Porphyrin-Based sp² Carbon-Conjugated Covalent Organic Framework for Heterogeneous Photocatalysis. *Angew. Chem., Int. Ed.* **2019**, *58* (19), 6430–6434.
- (13) Yuan, C.; Jia, W.; Yu, Z.; Li, Y.; Zi, M.; Yuan, L.-M.; Cui, Y. Are Highly Stable Covalent Organic Frameworks the Key to Universal Chiral Stationary Phases for Liquid and Gas Chromatographic Separations? *J. Am. Chem. Soc.* **2022**, *144* (2), 891–900.
- (14) Wang, S.; Li, X.-X.; Da, L.; Wang, Y.; Xiang, Z.; Wang, W.; Zhang, Y.-B.; Cao, D. A Three-Dimensional sp² Carbon-Conjugated

- Covalent Organic Framework. *J. Am. Chem. Soc.* **2021**, *143* (38), 15562–15566.
- (15) Jin, E.; Asada, M.; Xu, Q.; Dalapati, S.; Addicoat, M. A.; Brady, M. A.; Xu, H.; Nakamura, T.; Heine, T.; Chen, Q.; Jiang, D. Two-dimensional sp^2 carbon-conjugated covalent organic frameworks. *Science* **2017**, *357* (6352), 673–676.
- (16) Zhang, Q.; Sun, Y.; Li, H.; Tang, K.; Zhong, Y.-W.; Wang, D.; Guo, Y.; Liu, Y. Synthesis of Two-Dimensional C–C Bonded Truxene-Based Covalent Organic Frameworks by Irreversible Brønsted Acid-Catalyzed Aldol Cyclotrimerization. *Research* **2021**, *2021*, No. 9790705.
- (17) Kuhn, P.; Antonietti, M.; Thomas, A. Porous, Covalent Triazine-Based Frameworks Prepared by Ionothermal Synthesis. *Angew. Chem., Int. Ed.* **2008**, *47* (18), 3450–3453.
- (18) Wang, K.; Yang, L.-M.; Wang, X.; Guo, L.; Cheng, G.; Zhang, C.; Jin, S.; Tan, B.; Cooper, A. Covalent Triazine Frameworks via a Low-Temperature Polycondensation Approach. *Angew. Chem., Int. Ed.* **2017**, *56* (45), 14149–14153.
- (19) Sun, T.; Liang, Y.; Xu, Y. Rapid, Ordered Polymerization of Crystalline Semiconducting Covalent Triazine Frameworks. *Angew. Chem., Int. Ed.* **2022**, *61* (4), No. e202113926.
- (20) Vitaku, E.; Gannett, C. N.; Carpenter, K. L.; Shen, L.; Abruña, H. D.; Dichtel, W. R. Phenazine-Based Covalent Organic Framework Cathode Materials with High Energy and Power Densities. *J. Am. Chem. Soc.* **2020**, *142* (1), 16–20.
- (21) Huang, N.; Lee, K. H.; Yue, Y.; Xu, X.; Irle, S.; Jiang, Q.; Jiang, D. A Stable and Conductive Metallophthalocyanine Framework for Electrocatalytic Carbon Dioxide Reduction in Water. *Angew. Chem., Int. Ed.* **2020**, *59* (38), 16587–16593.
- (22) Waller, P. J.; AlFaraj, Y. S.; Diercks, C. S.; Jarenwattananon, N. N.; Yaghi, O. M. Conversion of Imine to Oxazole and Thiazole Linkages in Covalent Organic Frameworks. *J. Am. Chem. Soc.* **2018**, *140* (29), 9099–9103.
- (23) Seo, J.-M.; Noh, H.-J.; Jeong, H. Y.; Baek, J.-B. Converting Unstable Imine-Linked Network into Stable Aromatic Benzoxazole-Linked One via Post-oxidative Cyclization. *J. Am. Chem. Soc.* **2019**, *141* (30), 11786–11790.
- (24) Zhang, B.; Wei, M.; Mao, H.; Pei, X.; Alshimiri, S. A.; Reimer, J. A.; Yaghi, O. M. Crystalline Dioxin-Linked Covalent Organic Frameworks from Irreversible Reactions. *J. Am. Chem. Soc.* **2018**, *140* (40), 12715–12719.
- (25) Lu, M.; Zhang, M.; Liu, C.-G.; Liu, J.; Shang, L.-J.; Wang, M.; Chang, J.-N.; Li, S.-L.; Lan, Y.-Q. Stable Dioxin-Linked Metallophthalocyanine Covalent Organic Frameworks (COFs) as Photo-Coupled Electrocatalysts for CO₂ Reduction. *Angew. Chem., Int. Ed.* **2021**, *60* (9), 4864–4871.
- (26) Guan, X.; Li, H.; Ma, Y.; Xue, M.; Fang, Q.; Yan, Y.; Valtchev, V.; Qiu, S. Chemically stable polyarylether-based covalent organic frameworks. *Nat. Chem.* **2019**, *11* (6), 587–594.
- (27) Rose, M.; Klein, N.; Senkovska, I.; Schrage, C.; Wollmann, P.; Böhlmann, W.; Böhrringer, B.; Fichtner, S.; Kaskel, S. A new route to porous monolithic organic frameworks via cyclotrimerization. *J. Mater. Chem.* **2011**, *21* (3), 711–716.
- (28) Lopez-Iglesias, B.; Suárez-García, F.; Aguilar-Lugo, C.; González Ortega, A.; Bartolomé, C.; Martínez-Illarduya, J. M.; de la Campa, J. G.; Lozano, A. E.; Álvarez, C. Microporous Polymer Networks for Carbon Capture Applications. *ACS Appl. Mater. Interfaces* **2018**, *10* (31), 26195–26205.
- (29) Zhu, X.; Tian, C.; Chai, S.; Nelson, K.; Han, K. S.; Hagaman, E. W.; Veith, G. M.; Mahurin, S. M.; Liu, H.; Dai, S. New Tricks for Old Molecules: Development and Application of Porous N-doped, Carbonaceous Membranes for CO₂ Separation. *Adv. Mater.* **2013**, *25* (30), 4152–4158.
- (30) Zhao, Y.-C.; Zhou, D.; Chen, Q.; Zhang, X.-J.; Bian, N.; Qi, A.-D.; Han, B.-H. Thionyl Chloride-Catalyzed Preparation of Microporous Organic Polymers through Aldol Condensation. *Macromolecules* **2011**, *44* (16), 6382–6388.
- (31) Gongora, A. E.; Xu, B.; Perry, W.; Okoye, C.; Riley, P.; Reyes, K. G.; Morgan, E. F.; Brown, K. A. A Bayesian experimental autonomous researcher for mechanical design. *Sci. Adv.* **2020**, *6* (15), No. eaaz1708.
- (32) Langner, S.; Häse, F.; Perea, J. D.; Stubhan, T.; Hauch, J.; Roch, L. M.; Heumueller, T.; Aspuru-Guzik, A.; Brabec, C. J. Beyond Ternary OPV: High-Throughput Experimentation and Self-Driving Laboratories Optimize Multicomponent Systems. *Adv. Mater.* **2020**, *32* (14), No. 1907801.
- (33) Wahab, H.; Jain, V.; Tyrrell, A. S.; Seas, M. A.; Kotthoff, L.; Johnson, P. A. Machine-learning-assisted fabrication: Bayesian optimization of laser-induced graphene patterning using in-situ Raman analysis. *Carbon* **2020**, *167*, 609–619.
- (34) Xie, Y.; Zhang, C.; Deng, H.; Zheng, B.; Su, J.-W.; Shutt, K.; Lin, J. Accelerate Synthesis of Metal–Organic Frameworks by a Robotic Platform and Bayesian Optimization. *ACS Appl. Mater. Interfaces* **2021**, *13* (45), 53485–53491.
- (35) Burger, B.; Maffettone, P. M.; Gusev, V. V.; Aitchison, C. M.; Bai, Y.; Wang, X.; Li, X.; Alston, B. M.; Li, B.; Clowes, R.; Rankin, N.; Harris, B.; Sprick, R. S.; Cooper, A. I. A mobile robotic chemist. *Nature* **2020**, *583* (7815), 237–241.
- (36) Häse, F.; Roch, L. M.; Kreisbeck, C.; Aspuru-Guzik, A. Phoenix: A Bayesian Optimizer for Chemistry. *ACS Cent. Sci.* **2018**, *4* (9), 1134–1145.
- (37) Jones, D. R.; Schonlau, M.; Welch, W. J. Efficient Global Optimization of Expensive Black-Box Functions. *J. Glob. Optim.* **1998**, *13* (4), 455–492.
- (38) Haase, F.; Lotsch, B. V. Solving the COF trilemma: towards crystalline, stable and functional covalent organic frameworks. *Chem. Soc. Rev.* **2020**, *49* (23), 8469–8500.
- (39) Alahakoon, S. B.; McCandless, G. T.; Karunathilake, A. A. K.; Thompson, C. M.; Smaldone, R. A. Enhanced Structural Organization in Covalent Organic Frameworks Through Fluorination. *Chem. Eur. J.* **2017**, *23* (18), 4255–4259.